Nano Res. 2012, 5(3): 145–151
DOI 10.1007/s12274-012-0191-8
Research Article

ISSN 1998-0124
CN 11-5974/O4

Symmetric Growth of Pt Ultrathin Nanowires from Dumbbell Nuclei for Use as Oxygen Reduction Catalysts

Qiangfeng Xiao[1], Mei Cai[2] (✉), Michael P. Balogh[2], Misle M. Tessema[1], and Yunfeng Lu[3] (✉)

[1] Optimal CAE Inc., 14492 Sheldon Road, Plymouth, MI 48170, USA
[2] General Motors Global Research and Development Center, 30500 Mound Road, Warren, MI 48090-9055, USA
[3] Chemical and Biomolecular Engineering Department, University of California, Los Angeles, CA 90095, USA

Received: 12 August 2011 / Revised: 25 September 2011 / Accepted: 2 December 2011

ABSTRACT

This work demonstrates the synthesis of Pt ultrathin nanowires assisted by chromium hexacarbonyl [$Cr(CO)_6$]. The nanowires exhibit a uniform diameter of 2–3 nm. The length can reach up to several microns. It was found that Cr species produced dumbbell-like nuclei which play a pivotal role in the formation of the Pt nanowires. Such Pt nanowires can be tuned to nanocubes by simply decreasing the concentration of [$Cr(CO)_6$]. Compared to a commercial Pt/C catalyst (45 wt%, Vulcan, Tanaka) and Pt black (fuel cell grade, Sigma), the synthesized Pt nanowires exhibit superior performance in electrocatalytic oxygen reduction with a specific activity of 0.368 mA/cm^2, which was 2.7 and 1.8 times greater than that of Pt/C (0.138 mA/cm^2) and Pt black (0.202 mA/cm^2), respectively. The mass activity of Pt nanowires (0.088 mA/μg) is 2.3 times that of Pt black (0.038 mA/μg) and comparable to that of Pt/C (0.085 mA/μg).

KEYWORDS

Nanowire, dumbbell, nanocube, chromium hexacarbonyl, fuel cell, oxygen reduction reaction

1. Introduction

Metallic nanocrystals have attracted growing interest due to their great potential applications in catalysis, plasmonics, sensing, and spectroscopy [1, 2]. Nanocrystals possess higher density of active atomic steps, edges, and kinks in comparison to their bulk counterparts, resulting in higher catalytic activity [3]. These properties are intimately related to the size and shape of the synthesized nanocrystals. Size control of nanocrystals can be achieved in most cases and has been extensively investigated. Shape control is emerging as an important frontier to explore due to its profound effect on the catalytic, optical, electronic, and magnetic properties [2]. Shape control can be generally achieved by using capping agents (e.g., polymers, surfactants) that selectively adsorb on specific facets and limits their growth. For instance, poly(vinylpyrrolidone) (PVP) has been widely employed in polyol reactions to produce noble metal (e.g., Ag, Au, Pt) cubes, cuboctahedra, and octahedra [4]. Surfactants, such as alkyl amines and acids, have also been demonstrated as powerful ligands to control the shape of metal colloids [5, 6].

Unlike the aforementioned methods, a novel method based on the introduction of a small amount of a reactive metal has recently been developed. The shape control is realized by mainly altering the kinetics of the nanocrystal growth. Puntes et al. reported the

Address correspondence to Mei Cai, mei.cai@gm.com; Yunfeng Lu, luucla@ucla.edu

synthesis of platinum cubes, polypods, cuboctahedra, and raspberries using cobalt nanocrystals [7]. However the resultant morphologies are usually limited to nanoparticles. Compared with zero-dimensional (0D) nanostructures, one-dimensional (1D) nanotubes, nanorods, or nanowires possess fewer lattice boundaries, fewer defect sites and longer segments of surface crystalline planes, and exhibit higher activity and durability. For example, acid-treated unsupported Pt ultrathin nanowires showed a specific activity of 1.45 mA/cm^2, which is 7 times higher than that of commercial carbon-supported Pt nanoparticles [8]. Carbon-supported multiarmed star-like platinum nanowires made in aqueous solution displayed high activity and durability [9]. A similar enhancement in oxygen reduction reaction (ORR) activity was observed for Pd nanorods prepared by electrodeposition [10]. Other 1D platinum group metal (PGM) catalysts including PtFe nanowires [11], Pd–Pt dendrites [12], and Pd–Pt core–shell nanowires [13] also showed outstanding performance. However, the synthesis of high quality ultrathin (sub 5 nm) Pt nanowires with high aspect ratio and uniform diameter is still challenging [14, 15]. Here we report the synthesis of Pt nanowires assisted by [$Cr(CO)_6$] and a study of their electrocatalytic properties in ORR. Such Pt nanowires can be readily tuned to nanocubes by decreasing the concentration of [$Cr(CO)_6$].

2. Experimental

2.1 Reagents

Platinum acetylacetonate ($Pt(acac)_2$, 97%), chromium hexacarbonyl (96%), chloroplatinic acid hexahydrate (ACS reagent), oleylamine (>70%), oleic acid (90%), mesitylene (98%), toluene (99.8%), *p*-xylene ($\geqslant$ 99%), 1-octadecene (90%), ethanol (200 proof), and chloroform ($\geqslant$ 99%) were purchased from Sigma Aldrich and used without further purification.

2.2 Synthesis of Pt nanowires

In a typical synthesis, 0.33 g of [$Cr(CO)_6$] was dissolved in 16 mL of an arene (e.g., toluene, xylene, or mesitylene) at 100 ˚C under Ar. 0.2 g of [$Pt(acac)_2$] was mixed with 20 mL of oleylamine and heated at 120 ˚C with stirring under Ar to form a clear light yellow solution. The freshly prepared [$Cr(CO)_6$] solution at 100 ˚C was then injected into the [$Pt(acac)_2$] solution. The color of the solution changed from light yellow, to brown, and then to black. The reaction was carried out at 120 ˚C for 30 min. The temperature was subsequently increased to 160 ˚C at a rate of 5 ˚C/min for another 30 min. Then the solution was cooled down to room temperature by removing the heating mantle and adding 40 mL of ethanol. The Pt nanowires were separated by centrifugation and decantation. Finally the product was redispersed in chloroform. Similar products were obtained when the temperature was directly raised to 160 ˚C after the injection of the [$Cr(CO)_6$] precursor instead of the two step procedure.

2.3 Preparation of working electrodes

For the commercial Pt/C catalyst (45 wt% Pt on Vulcan XC-72 carbon support, Tanaka), an aqueous dispersion (1 mg/mL) was prepared and sonicated for 60 min. 20 μL of the dispersion was then transferred onto a glassy carbon rotating disk electrode (RDE) with a geometric area of 0.196 cm^2. For the Pt nanocubes and nanowires, 20 μL of the chloroform solution was transferred onto the RDE in the same way as the Pt/C catalyst and the mass of catalyst was determined using inductively coupled plasma optical emission spectroscopy (ICP-OES) analysis. The Pt nanocubes and nanowires were treated with plasma (79% Ar and 21% O_2, Model 1020 Plasma Cleaner, E.A. Fischione Instruments) for 5 min to remove the surfactants. After the electrode was dried in air, 20 μL of 0.05 wt% Nafion solution was employed to cover the electrode. The electrochemical measurements were carried out until the Nafion solution was completely dried.

2.4 Characterization

Transmission electron microscopy (TEM) and scanning TEM images were obtained using a JEOL JEM 2100F microscope at 200 kV. X-ray diffraction (XRD) patterns were obtained on Bruker D8 Advance with Cu Kα radiation (λ = 1.5418 Å). Composition analysis of Pt nanocubes and nanowires was carried out by both energy dispersive X-ray spectroscopy (EDS) using a scanning electron microscope (SEM) (Hitachi S4800)

and ICP-OES on a Varian 725-ES spectrometer. All the electrochemical measurements were recorded on a Voltalab (PGZ 100) potentiostat.

3. Results and discussion

Figure 1(a) shows a typical low magnification TEM image of the as synthesized nanowires prepared with 93.75 mmol/L [$Cr(CO)_6$] and 25 mmol/L [$Pt(acac)_2$] at 120 ˚C for 30 min and at 160 ˚C for another 30 min under Ar. The diameter of these nanowires is about 2–3 nm. Some nanowires can reach several micrometers in length, as indicated by the scanning TEM image in Fig. 1(b). Note that both ends of individual nanowires have a cattail-like morphology. A high-resolution transmission electron microscope (HRTEM) image (Fig. 1(c)) shows the presence of both single crystalline and polycrystalline nanowires. The measured inter-fringe distance of the single crystal is about 0.23 nm, which corresponds to the (111) planes of Pt. This indicates that the nanowires grow along the [111] direction. Similar to ultrathin Au nanowires [16], such nanowires were observed to break into fragments upon exposure to the electron beam irradiation, which induces electron beam annealing (Fig. S-1 in the Electronic Supplementary Material (ESM)). The crystal structure of the Pt nanowires was characterized by XRD. The pattern in Fig. 1(d) indicates that they possess a highly crystalline face-centered cubic (fcc) phase with space group $Fm\bar{3}m$, and their lattice parameter is identical to that of pure Pt. The chemical composition determined by ICP-OES analysis indicates there is 0.6 wt% Cr (relative to 99.4 wt% Pt) in the nanowires after the nanowires were thoroughly purified with hexane and ethanol. This trace amount of Cr is beyond the sensitivity of EDS analysis and Cr was not observed (Fig. S-2 in the ESM). These results suggest that Cr species serve as reducing and shape-directing agents rather than doping into the Pt lattice to form an alloy. Different from the case of PtFe nanowires [11], the length of the Pt nanowires cannot be tuned by the addition of solvent. Increasing the amount of 1-octadecene (ODE) resulted in more Pt nanoparticles and fewer nanowires (Fig. S-3 in the ESM).

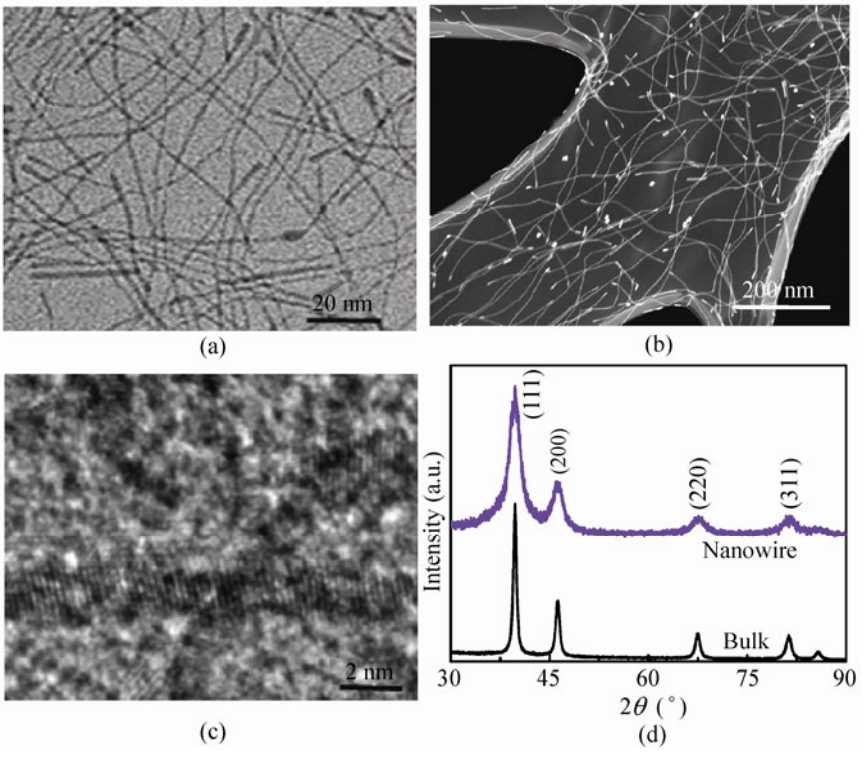

Figure 1 (a) TEM image, (b) scanning TEM image, (c) HRTEM, and (d) XRD pattern of the Pt nanowires

Such Pt nanowires can be tuned to nanocubes by simply decreasing the concentration of $[Cr(CO)_6]$ from 93.75 mmol/L to 10.42 mmol/L. When the concentration was within the above range, a mixture of nanocubes and nanowires was formed. Figure 2(a) shows a typical low magnification TEM image of the as synthesized nanocubes. They are nearly monodisperse and possess an average edge length of 6 nm. A HRTEM image of a single nanocube (Fig. 2(b)) shows its highly crystalline structures. The measured *d* spacing is about 0.195 nm, close to the lattice spacing of the (200) planes (0.196 nm) in the pure fcc Pt crystal. According to the Scherrer equation, the crystallite size was estimated to be 5.6 nm, which is quite consistent with the TEM results. The chemical composition determined by EDS and ICP-OES analysis did not find the presence of Cr in the nanocubes within instrumental detection limits. Note that such nanocubes were obtained by using oleylamine rather than using the combination of oleic acid and oleylamine as previously reported for Pt and PtM (M = Ni, Mn, Co, Fe) nanocubes [17–20].

To explore the possible growth mechanism of the nanowires, the effect of varying the concentrations of $[Cr(CO)_6]$ and $[Pt(acac)_2]$, addition of ligands and the nature of the Pt source on the final shape of the product were investigated. In the case of nanowire synthesis, when only $[Cr(CO)_6]$ was used, no particles were obtained. However, without $[Cr(CO)_6]$, the resulting nanocrystals possess polypod structures (Fig. 3(a)), whose branches have an average diameter of 2–3 nm and a length of 4–8 nm. When $[W(CO)_6]$ was used, only nanoparticles were obtained (Fig. S-4 in the ESM). If the concentration of $[Pt(acac)_2]$ was diluted 5 fold, both particles and nanowires (Fig. 3(b)) were produced. If oleylamine was replaced by oleic acid, the as-synthesized Pt nanoparticles tend to aggregate into ordered mesostructures (Fig. 3(c)) due to the weak capping capability of oleic acid. The Pt source also played an essential role in the shape control. For example, using H_2PtCl_6 produced only Pt nanoparticles with irregular shape (Fig. 3(d)). Overall, the combination of $[Pt(acac)_2]$–$[Cr(CO)_6]$–oleylamine provides great flexibility to tune the shape of the Pt nanocrystals. When the concentrations of both Pt and Cr precursor are high (e.g., $[Pt(acac)_2] \geqslant 25$ mmol/L and $[Cr(CO)_6] \geqslant 93.75$ mmol/L), nanowires can be formed, whilst lower concentrations of either Pt or Cr precursor (e.g., $[Pt(acac)_2] \leqslant 5$ mmol/L or $[Cr(CO)_6] \leqslant 10.42$ mmol/L) tend to produce Pt nanoparticles.

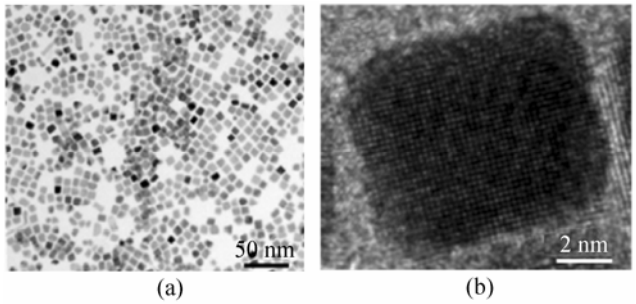

Figure 2 (a) TEM image and (b) HRTEM image of Pt nanocubes

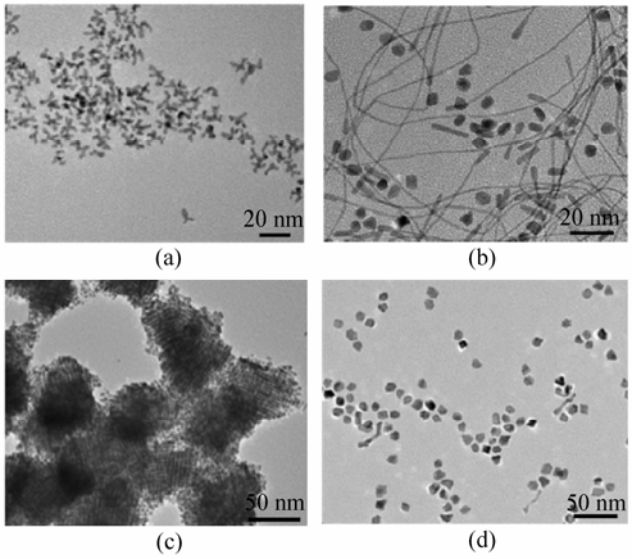

Figure 3 TEM images of (a) Pt polypods synthesized in the absence of $[Cr(CO)_6]$, (b) a mixture of nanoparticles and nanowires prepared by 5 fold dilution of $[Pt(acac)_2]$, (c) Pt ordered mesostructures prepared with oleic acid, and (d) Pt irregular nanoparticles prepared with chloroplatinic acid hexahydrate $[H_2PtCl_6{\cdot}6H_2O]$ as Pt source. All the reactions were carried out with the formation of Pt nanowires as a control reaction

The kinetic process of Pt nanowire formation was investigated by sampling at different reaction times. At a time of 1 min after the $[Cr(CO)_6]$ precursor was injected, two Pt nuclei were fused at the corners and dumbbell structures (Fig. 4(a)) had developed. Once these nuclei generated, the reduction of the Pt(Ⅱ) species was greatly accelerated by an autocatalytic process. After 3 min, the length of some nanowires reached more than 200 nm, as shown in Fig. 4(b). Note

that the Cr species play a pivotal role in the formation of dumbbell structures. When $Cr(CO)_6$ was replaced by $W(CO)_6$, no dumbbell structures were obtained.

Based on the results, the following growth mechanism of shape evolution can be proposed. When the concentrations of either Pt or Cr precursors are low, isolated nuclei are produced and finally grow into nanoparticles. When the concentrations of both Pt and Cr precursors increase, more nuclei are generated, therefore facilitating the formation of dumbbell structures. According to the study by Wang et al. [21], for faceted particles, ligands favorably passivate on facets rather than at edges or corners. As shown schematically in Fig. 4(c), the joint of a dumbbell then acts as a catalytic site and favors the addition of more Pt atoms due to the non-uniform distribution of the ligands on the surface, as well as interfacial strain. Subsequently this joint becomes autocatalytically elongated to form a nanowire. The exact role of the Cr species in the formation of nanowires needs to be further explored in order to completely understand the mechanism.

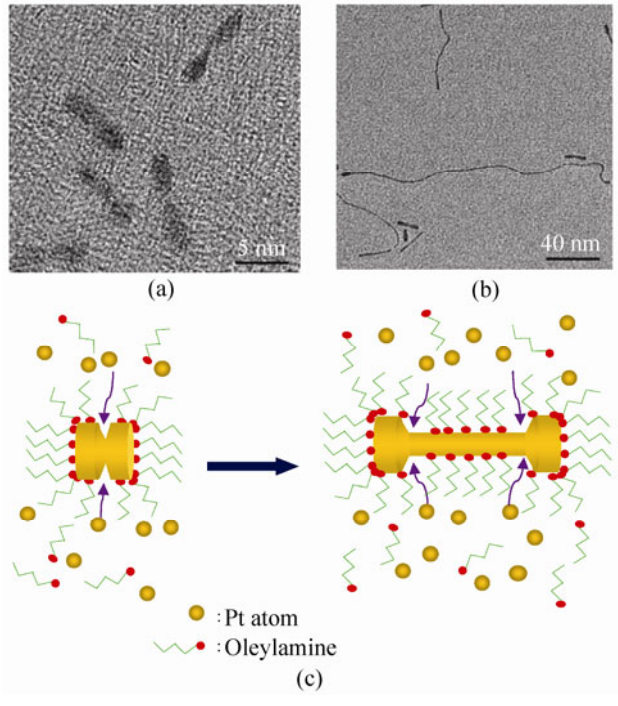

Figure 4 TEM images of (a) Pt dumbbells sampled at 1 min and (b) Pt nanowires sampled at 3 min during the synthesis of Pt nanowires after injection of $[Cr(CO)_6]$ precursor. (c) Schematic illustration of the mechanism of Pt nanowire formation

The catalytic activity of the synthesized nanocubes and nanowires was investigated by electrochemical measurements using Pt/C (45 wt%, Vulcan, Tanaka) and Pt black (fuel cell grade, Sigma) as benchmarks. The catalysts (Pt nanocubes, nanowires, Pt black, and Pt/C) were deposited onto glassy carbon with a geometric area of 0.196 cm^2 as the working electrode. A saturated calomel electrode (SCE) and a Pt wire wrapped with Pt mesh were employed as the reference and counter electrode, respectively. Figure 5(a) shows cyclic voltammograms of the catalysts obtained in 0.1 mol/L $HClO_4$ electrolyte purged with ultrahigh purity Ar at room temperature with a potential sweep rate of 20 mV/s. Similar to the features for Pt black and Pt/C, both nanocubes and nanowires exhibit cyclic voltammograms with hydrogen adsorption and desorption regions, a double-layer capacitance region, and the formation and reduction of Pt oxide. This indicates that the surfactants had been effectively removed by plasma treatment. The electrochemically active surface area (ECSA) was calculated by integrating the area under the curves for Pt hydride formation and removal after double-layer correction and assuming a value of 210 μC/cm^2 for the adsorption of one hydrogen monolayer. The ECSA of Pt nanowires reached 24 m^2/g which is comparable to Pt nanowires prepared using mesoporous silica as a template [22]. Figure 5(b) illustrates the ORR polarization curves normalized to surface area of the catalysts with O_2-saturated electrolytes at room temperature and rotation speed of 1600 rpm with a potential sweep rate of 5 mV/s. The specific catalytic activity was taken as the kinetic current at 0.9 V normalized to the ECSA. Pt nanocubes exhibit a specific activity of 0.278 mA/cm^2 and a mass activity of 0.33 mA/μg, close to the reported results [23]. The specific activity of Pt nanowires (0.368 mA/cm^2) is 2.7 times that of Pt/C (0.138 mA/cm^2) and 1.8 times that of Pt black (0.202 mA/cm^2). The mass activity of Pt nanowires (0.088 mA/μg) is 2.3 times that of Pt black (0.038 mA/μg) and comparable to that of Pt/C (0.085 mA/μg). Such enhancement can be ascribed to the surface contraction associated with the ultrathin diameter [8]. Improved stability of the Pt nanowires can be expected because no additional carbon support is required.

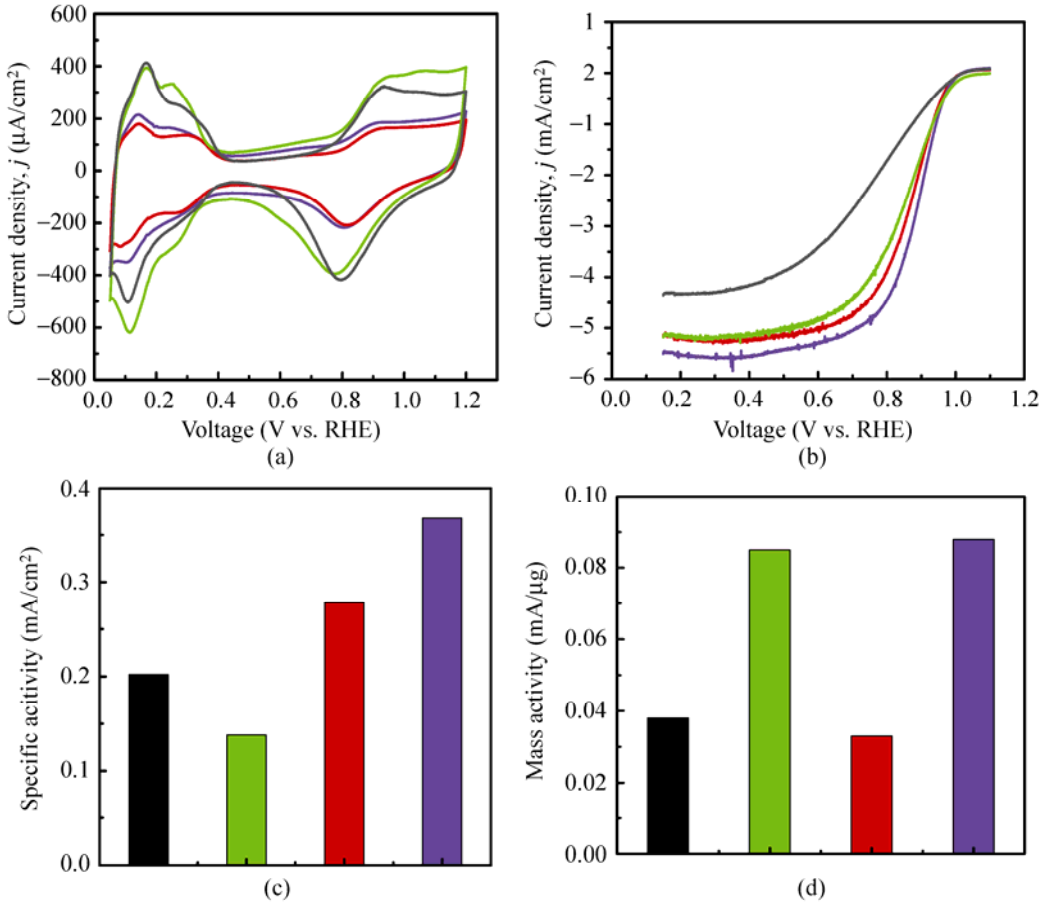

Figure 5 (a) CV curves recorded at room temperature in an Ar-purged 0.1 mol/L $HClO_4$ solution with a sweep rate of 20 mV/s. (b) ORR polarization curves for the Pt nanowires (purple), nanocubes (red), Pt black (black), and Pt/C catalyst (green) recorded at room temperature in an O_2-saturated 0.1 mol/L $HClO_4$ solution with a sweep rate of 5 mV/s and a rotation rate of 1600 rpm. (c) Specific activity and (d) mass activity at 0.9 V versus the standard hydrogen electrode (SHE) for the four catalysts

4. Conclusions

We have successfully synthesized Pt ultrathin nanowires with a uniform diameter of 2–3 nm and high aspect ratio by symmetric growth from dumbbell nuclei. $[Cr(CO)_6]$ plays a pivotal role in the formation of these dumbbell nuclei. These nanowires exhibit superior catalytic properties compared with Pt nanocubes and commercial catalysts. Considering that $[Cr(CO)_6]$ acts as both reducing and shape directing agents, we believe that this method opens the door to synthesize Pt-based alloy ultrathin nanowires with controllable composition.

Acknowledgements

This work was supported by GM internal funding. We acknowledge Dr. Zhongyi Liu and Dr. Ratandeep S. Kukreja for great help with TEM and scanning TEM measurements. We would also like to thank Nick Irish for the ICP-OES analysis and Marty Ruthkosky for the help in setting up some instruments.

Electronic Supplementary Material: TEM and EDS of the Pt nanocrystals with other shapes are available in the online version of this article at http://dx.doi.org/10.1007/s12274-012-0191-8.

References

[1] Lee, Y.; Loew, A.; Sun, S. H. Surface- and structure-dependent catalytic activity of Au nanoparticles for oxygen reduction reaction. *Chem. Mater.* **2010**, *22*, 755–761.

[2] Tao, A. R.; Habas, S.; Yang, P. D. Shape control of colloidal metal nanocrystals. *Small* **2008**, *4*, 310–325.

[3] Ahmadi, T. S.; Wang, Z. L.; Green, T. C.; Henglein, A.; El-Sayed, M. A. Shape-controlled synthesis of colloidal platinum nanoparticles. *Science* **1996**, *272*, 1924–1926.

[4] Rao, C. N. R.; Vivekchand, S. R. C.; Biswasa, K.; Govindaraja, A. Synthesis of inorganic nanomaterials. *Dalton Trans.* **2007**, 3728–3749.

[5] Zhang, J.; Fang, J. Y. A general strategy for preparation of Pt 3d-transition metal (Co, Fe, Ni) nanocubes. *J. Am. Chem. Soc.* **2009**, *131*, 18543–18547.

[6] Peng, Z. M.; Yang, H. Synthesis and oxygen reduction electrocatalytic property of Pt-on-Pd bimetallic heteronanostructures. *J. Am. Chem. Soc.* **2009**, *131*, 7542–7543.

[7] Lim, S. I.; Ojea-Jimenez, I.; Varon, M.; Casals, E.; Arbiol, J.; Puntes, V. Synthesis of platinum cubes, polypods, cuboctahedrons, and raspberries assisted by cobalt nanocrystals. *Nano Lett.* **2010**, *10*, 964–973.

[8] Koenigsmann, C.; Zhou, W.; Adzic, R. R.; Sutter, E.; Wong, S. S. Size-dependent enhancement of electrocatalytic performance in relatively defect-free, processed ultrathin platinum nanowires. *Nano Lett.* **2010**, *10*, 2806–2811.

[9] Sun, S. H.; Zhang, G. X.; Geng, D. H.; Chen, Y. G.; Li, R. Y.; Cai, M.; Sun X. L. A highly durable platinum nanocatalyst for proton exchange membrane fuel cells: Multiarmed starlike nanowire single crystal. *Angew. Chem. Int. Ed.* **2011**, *123*, 442–446.

[10] Xiao, L.; Zhuang, L.; Liu, Y.; Lu, J.; Abruñhen, H. D. Activating Pd by morphology tailoring for oxygen reduction. *J. Am. Chem. Soc.* **2009**, *131*, 602–608.

[11] Zhang, Z. Y.; Li, M. J.; Wu, Z. L.; Li, W. Z. Ultra-thin PtFe-nanowires as durable electrocatalysts for fuel cells. *Nanotechnology* **2011**, *22*, 015602.

[12] Lim, B.; Jiang, M. J.; Camargo, P. H. C.; Cho, E. C.; Tao, J.; Lu, X. M.; Zhu, Y. M.; Xia, Y. N. Pd–Pt bimetallic nanodendrites with high activity for oxygen reduction. *Science* **2009**, *324*, 1302–1305.

[13] Koenigsmann, C.; Santulli, A. C.; Gong, K. P.; Vukmirovic, M. B.; Zhou, W. P.; Sutter, E.; Wong, S. S.; Adzic, R. R. Enhanced electrocatalytic performance of processed, ultrathin, supported Pd–Pt core–shell nanowire catalysts for the oxygen reduction reaction. *J. Am. Chem. Soc.* **2011**, *133*, 9783–9795.

[14] Chen, J.; Herricks, T.; Geissler, M.; Xia, Y. Single-crystal nanowires of platinum can be synthesized by controlling the reaction rate of a polyol process. *J. Am. Chem. Soc.* **2004**, *126*, 10854–10855.

[15] Sun, S. H.; Zhang, G. X.; Zhong, Y.; Hao, H.; Li, R. Y.; Zhou, X. R.; Sun, X. L. Ultrathin single crystal Pt nanowires grown on N-doped carbon nanotubes. *Chem. Commun.* **2009**, 7048–7050.

[16] Wang, C.; Sun, S. H. Facile synthesis of ultrathin and single-crystalline Au nanowires. *Chem. Asian J.* **2009**, *4*, 1028–1034.

[17] Wang, C.; Hou, Y. L.; Kim, J.; Sun, S. H. A general strategy for synthesizing FePt nanowires and nanorods. *Angew. Chem. Int. Ed.* **2007**, *46*, 6333–6335.

[18] Wang, C.; Daimon, H.; Lee, Y. M.; Kim, J. M.; Sun, S. H. Synthesis of monodisperse Pt nanocubes and their enhanced catalysis for oxygen reduction. *J. Am. Chem. Soc.* **2007**, *129*, 6974–6975.

[19] Kang, Y. J.; Murray, C. B. Synthesis and electrocatalytic properties of cubic Mn–Pt nanocrystals (nanocubes*). J. Am. Chem. Soc.* **2010**, *132*, 7568–7569.

[20] Chen, M.; Kim, J. M.; Liu, J. P.; Fan, H. Y.; Sun, S. H. Synthesis of FePt nanocubes and their oriented self-assembly. *J. Am. Chem. Soc.* **2006**, *128*, 7132–7133.

[21] Wang, Z. L. Structural analysis of self-assembling nanocrystal superlattices. *Adv. Mater.* **1998**, *10*, 13–30.

[22] Wang, D. H.; Luo, H. M.; Kou, R.; Gil, M. P.; Xiao, S. G.; Golub, V. O.; Yang, Z. Z.; Brinker, C. J.; Lu, Y. F. A general route to macroscopic hierarchical 3D nanowire networks. *Angew. Chem. Int. Ed.* **2004**, *116*, 6295–6299.

[23] Zhang, J.; Yang, H. Z.; Fang, J. Y.; Zou, S. Z. Synthesis and oxygen reduction activity of shape-controlled Pt_3Ni nanopolyhedra. *Nano Lett.* **2010**, *10*, 638–644.